

STRENGTHENING WITH FRP BARS OF URM WALLS SUBJECT TO OUT-OF-PLANE LOADS

Nestore Galati
University of Missouri-Rolla, USA
Gustavo J. Tumialan
Simpson Gumpertz and Heger, USA
Stefano Secondin
University of Padua - Italy
Antonio Nanni
University of Missouri-Rolla, USA

For the retrofitting of the civil infrastructure, an alternative to Fiber Reinforced Polymer (FRP) externally-bonded laminates is the use near surface mounted (NSM) FRP bars. This technique consists of placing a bar in a groove cut into the surface of the member being strengthened. The FRP bar may be embedded in an epoxy- or cementitious-based paste, which transfers stresses between the substrate and the bar. The successful use of NSM FRP bars in the strengthening of concrete members has been extended to unreinforced masonry (URM) walls, one of the building components most prone to failure during a seismic event. This paper presents the results of an experimental program on the flexural behaviour of URM walls strengthened with (NSM) FRP bars. A total of fifteen URM walls reinforced with NSM FRP bars were tested. The specimens were strengthened with different amounts of reinforcement to observe their improved performance and the mode of failure. The influence of the bar shape (i.e. circular vs. rectangular), dimension of the groove and type of embedding material (i.e. epoxy or cementitious-based paste), were studied. Two types of FRP fabrics, glass (GFRP) and carbon (CFRP), were used as externally bonded reinforcement to provide the benchmark. Strength and pseudo-ductility of URM walls were significantly increased by strengthening with FRP bars. Based on experimental evidence and on the data found in the literature, the paper provides criteria that can be used in the development of design guidelines.

INTRODUCTION

Unreinforced masonry (URM) walls are prone to failure when subjected to overstress caused by out-of-plane and in-plane loads. Externally bonded FRP laminates have been successfully used to increase the flexural and/or the shear capacity of reinforced concrete (RC) and masonry members. The use of near-surface-mounted (NSM) FRP bars is an attractive method for increasing flexural and shear strength of deficient RC members (De Lorenzis et al., 2000) and masonry walls and, in certain cases, can be more convenient than using FRP laminates (i.e. anchoring requirements, aesthetics requirements).

A previous investigation has shown the effectiveness of FRP bars for increasing the flexural capacity of URM walls (Hamid, 1996). In that investigation, the FRP reinforcement was internally placed, this technique demanded the cutting of slots at the top course of the wall to place the bars, drilling of holes to pump grout, and grouting. The successful use of near-surface-mounted (NSM) bars for improving the flexural capacity of RC members led to extending their potential use for the strengthening of URM walls. The use of NSM FRP bars is attractive since their

application does not require any surface preparation work and requires minimal installation time.

This paper presents an experimental program on 15 URM walls reinforced with FRP bars using the NSM technique and subjected to out-of-plane loads. The influence of five parameters was investigated: type and amount of FRP reinforcement, shape of the FRP bars (i.e. circular or rectangular), groove size and type of embedding material (i.e. epoxy- or cementitious- paste). Also the effectiveness of the FRP reinforcement for masonry panels having a running or a stack pattern bond type was studied. In addition, based on experimental evidence and on experimental results available in the literature (Turco, 2002 and Fortes et al., 2002), this paper provides criteria that can be used in the development of design guidelines.

TEST MATRIX

As shown in Table 1, fifteen masonry walls were manufactured for this experimental program. Three specimens were built with clay bricks. The remaining twelve were built with concrete blocks. The nominal dimensions of these walls were 1.22 m (48 in) by 0.61 m (24 in); their overall thickness was 95 mm ($3\frac{3}{4}$ in) for clay specimens.

Table 1- Test Matrix

Specimen Designation	Thickness of the Specimen mm (in)	Bar Type	Groove Dimension	Embedment Material
CO1-GTE1	143 ($5\frac{3}{4}$)	GFRP Rectangular		
CO1-GTE2	143 ($5\frac{3}{4}$)	GFRP Rectangular	Rectangular Groove	Epoxy
CL1-GTE1	95 ($3\frac{3}{4}$)	GFRP Rectangular	17x3 (0.67x0.12)	
CL1-GTE2	95 ($3\frac{3}{4}$)	GFRP Rectangular		
CL2-CTE1	95 ($3\frac{3}{4}$)	CFRP Rectangular		
CO2-GRE21	92 ($3\frac{5}{8}$)	GFRP Circular	Square Groove 2.25 the Diameter of the Bar	Epoxy
CO2-GRE22	92 ($3\frac{5}{8}$)	GFRP Circular	14.3 mm (0.56 in.)	
CO2-GRE23	92 ($3\frac{5}{8}$)	GFRP Circular		
CO2-GRC31	92 ($3\frac{5}{8}$)	GFRP Circular	Square Groove 2.25 the Diameter of the Bar	Cementitious Paste
CO2-GRC32	92 ($3\frac{5}{8}$)	GFRP Circular	21.4 mm (0.84 in.)	
CO2-GRC33	92 ($3\frac{5}{8}$)	GFRP Circular		
CO2-GRE21-SJ	92 ($3\frac{5}{8}$)	GFRP Circular	Square Groove 1.5 the Diameter of the Bar	Epoxy
CO2-GRE22-SJ	92 ($3\frac{5}{8}$)	GFRP Circular	9.5 mm (0.37 in.)	
CO2-GRE21-S	92 ($3\frac{5}{8}$)	GFRP Circular		
CO2-GRE22-S	92 ($3\frac{5}{8}$)	GFRP Circular		

In the case of the concrete masonry walls the thickness varied from 92 mm ($3\frac{5}{8}$ in.) to 143 mm ($5\frac{3}{4}$ in.) (See Figure 1). The walls were constructed using a Type N mortar. All the joints were finished flush with the surface of the masonry unit. All specimens were allowed to cure for at least 28 days before testing. The specimens were strengthened, using the NSM technique, with 6.35 mm ($\frac{2}{8}$ in.) and 9.53 mm ($\frac{3}{8}$ in.) diameter deformed GFRP bars and with 2 x 15 mm (0.080 x 0.60 in.) GFRP or with 2 x 16 mm (0.08 x 0.63 in.) CFRP rectangular bars.

A two-part code was used to identify the specimens. The first part of the code identifies the parent material. Thus, the first two characters identify the type of masonry used “CO” for concrete masonry and “CL” for clay masonry. Since the specimens were constructed using bricks or blocks coming from different stocks, the third number in the code is to identify the stock of the material. From Table 1 it can be observed that four different types of masonry were used: two for the clay walls (CL1 and CL2), and two for the concrete walls (CO1 and CO2).

The second part of the code identifies the type and amount of FRP reinforcement. In particular, the first character is the type of FRP reinforcement used: “G” for GFRP and “C” for CFRP. The second character represents the cross section of the bar used: “T” for rectangular bar and “R” for circular bar. The third character identifies the type of embedding material: “E” for epoxy paste and “C” for latex modified (cementitious grout). For the specimens using rectangular bars the last number represents the number of bars used for the strengthening. For the other specimens, the two numbers following the character “E” or “C” represent the diameter in eighth of an inches and the number of NSM Bars per specimen respectively. The final character “S” or “SJ” indicates that the masonry panels were built with a stack pattern bond type with reinforcement crossing the blocks or placed in the vertical joints respectively (See Figure 2).

Thus CO2-GRE21-SJ, refers to a concrete masonry panel, built with a stack pattern bond type, strengthened with one 6.35 mm ($\frac{2}{8}$ in.) diameter GFRP bar embedded in epoxy-based paste and placed in the vertical joints.



a) Stack Bond Pattern



b) Running Bond Pattern

Figure 1 - Test Specimens

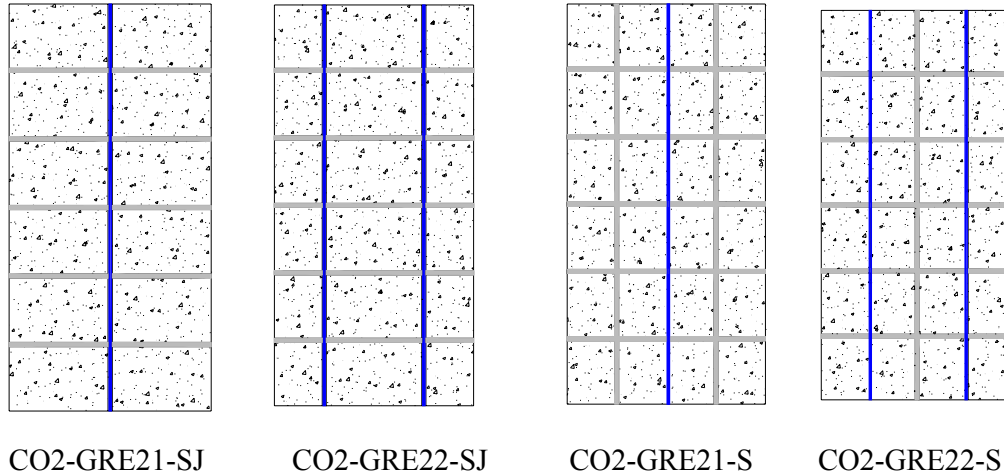


Figure 2 - Reinforcement Scheme for Specimens Built with a Stack Pattern Bond Type Having Reinforcement Crossing the Blocks (CO2-GRExy-S), or Placed in the Vertical Joints (CO2-GRExy-S)

MATERIAL PROPERTIES

Tests were performed to characterize the mechanical properties of the materials used in this investigation. The average compressive strengths of concrete and clay masonry obtained from the testing of prisms (ASTM C1314) are presented in Table 2.

A mortar Type N was used for the walls construction; standard mortar specimens were tested according to ASTM C109. An average value of 7.6 MPa (1100 psi) at an age of 28 days was found.

Table 2 - Compressive Strength of Masonry Walls

Dimensions of Masonry Units mm (in.)	Masonry Type	Specimen Code	Compressive Strength MPa (ksi)
150 x 200 x 400 (5 5/8" x 7 7/8" x 15 3/4")	Concrete	CO1	11.4 (1.6)
100 x 200 x 400 (3 5/8" x 7 7/8" x 15 3/4")	Concrete	CO2	10.5 (1.5)
100 x 200 x 65 (3 3/4" x 2 1/2" x 7 7/8")	Clay	CL1	19.43 (2.8)
100 x 200 x 65 (3 3/4" x 2 1/2" x 7 7/8")	Clay	CL2	15.78 (2.3)

Tensile tests were performed on FRP bars to determine their engineering properties, which are related to fiber content. The average tensile strength, ultimate strain and modulus of elasticity obtained from the testing of the specimens (ASTM D3039) are presented in Table 3. Details of coupon fabrication and testing procedure are shown elsewhere (Secondin 2003).

Table 3 - Mechanical Properties of FRP Bars

Bar Type	Dimensions of the Bar	Average Maximum Strain %	Average Maximum Stress MPa (ksi)	Average Elastic Modulus MPa (ksi)
#2 GFRP Bar	Nominal Diameter 6.35 mm (0.250 in.)	1.78	824.5 (119.6)	50163 (7276)
#3 GFRP Bar	Nominal Diameter 9.53 mm (0.375 in.)	1.85	760.0 (110.0)	40800 (5920)
GFRP Rectangular Bar	2.06 mm x 15.21 mm (0.081" x 0.599")	2.5	1101.7 (159.8)	44000 (6382)
CFRP Rectangular Bar	2.06 mm x 15.21 mm (0.081" x 0.599")	0.98	1392.4 (201.9)	142740 (20702)

Splitting tensile tests (ASTM C496) were performed on the epoxy-based and on the cementitious-based embedding material used. The splitting tensile strength was found to be 3.58 MPa (0.518 ksi) after 7 days and 5.59 MPa (0.81 ksi) after 28 days in the case of latex modified cementitious paste, and 16.31 MPa (2.36 ksi) after 7 days and 18.54 MPa (2.7 ksi) after 28 days in the case of epoxy-based paste.

TEST SETUP

The masonry specimens were tested under four-points bending (See Figure 3). Loads were applied by 50.8 x 609.6 x 12.7 mm (2 x 24 x ½ in.) steel plates to the external face of the wall. Their distance was 101.6 mm (4 in.) from the midspan. The loads were generated by means of a 12 ton hydraulic jack reacting against a steel frame. Linear Variable Displacement Transducers (LVDTs) were positioned in the middle of the walls to measure the midspan deflection during the tests.

The load was applied in cycles of loading and unloading. An initial cycle for a low load was performed in every wall to verify that both the mechanical and electronic equipment were working properly.

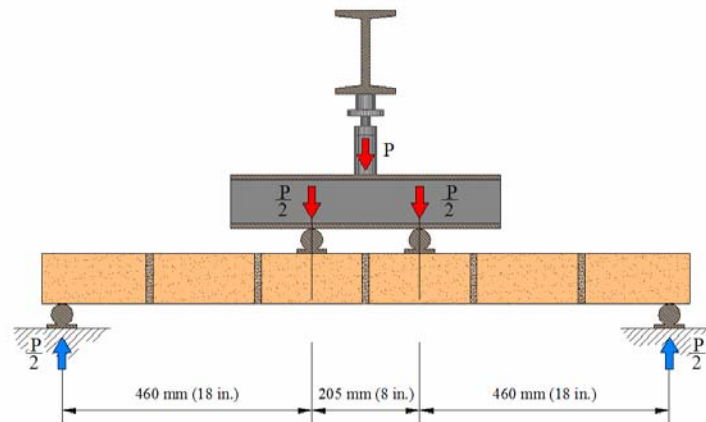


Figure 3 - Test Setup Scheme

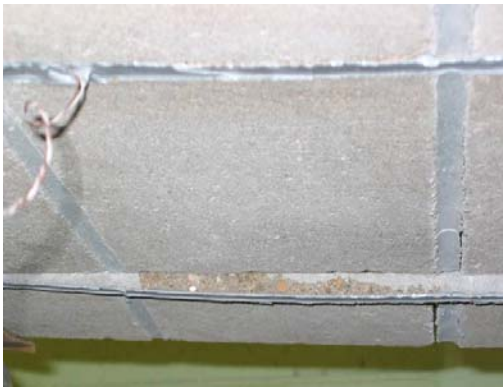
TEST RESULTS

Modes of Failure

The walls exhibited three different modes of failure (See Figure 4): (1) Debonding of the FRP reinforcement from the masonry substrate; (2) Flexural failure (i.e. crushing of the masonry in compression or rupture of the FRP in tension); and, (3) Shear failure of the masonry at the supports.

FRP Debonding.

This was the most frequent mode of failure. Initial flexural cracks were primarily located at the mortar joints (See Figure 4-a). A cracking noise during the test revealed a progressive cracking of the embedding paste. Since the tensile stresses at the mortar joints were being taken by the FRP reinforcement, a redistribution of stresses occurred. As a consequence, cracks developed in the masonry units oriented at 45° (see Figure 4-b) or in the head mortar joints. Some of these cracks followed the embedding paste and masonry interface causing debonding and subsequent wall failure.



a) FRP Bar Debonding (CO2-GRC32)



b) FRP Debonding: Formation of the 45° Cracks at the Head Joints (CO2-GRC31)



c) Splitting Cracks in the Embedding Material (CO2-GRE22)



d) Flexural – Shear Failure (CO2-GRC33)

Figure 4 - Modes of Failure

Due to the smoothness of the rectangular bars, for some of the specimens reinforced with rectangular bars debonding was caused by sliding of the bar inside the epoxy.

For specimens having a deep groove, debonding was caused by splitting of the embedding material (See Figure 4-c).

Flexural Failure.

After developing flexural cracks primarily located at the mortar joints, a wall failed by either rupture of the FRP reinforcement or masonry crushing. FRP rupture occurred at midspan and was observed for the specimens CO2-GRE21 and CO2-GRE22.

Shear Failure.

Cracking started with the development of fine vertical cracks at the maximum bending region. Thereafter flexural-shear failure was observed. It was oriented at approximately 45°. In the flexural-shear mode, shear forces transmitted over the crack caused a differential displacement in the shear plane, which resulted in FRP debonding (See Figure 4-d).

Discussion of Results

Figure 5 shows the Moment vs. Deflection Curves for the six series. It can be observed that the strength and stiffness of the FRP strengthened walls increased dramatically when comparing them to a URM specimen.

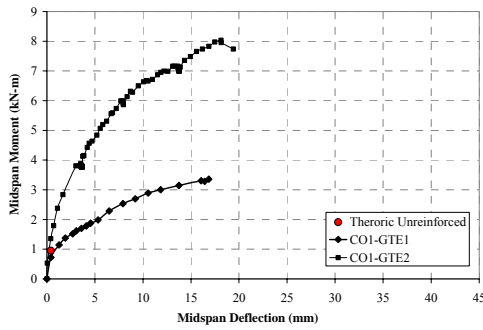
The nominal moments at cracking for the un-strengthened specimens were calculated considering the Masonry Standards Joint Committee recommendations (MSJC-02). From the graphs in Figure 5 they can be stated increments ranging from 4 to 14 times of the original masonry capacity. Since masonry possesses a significant amount of variability attributed to labour and materials, this range of values should be taken simply as a reference.

Table 4 reports the test results. The experimental results have been expressed as a function of the amount of reinforcement, ρ_f , defined as $\text{Area}_{\text{FRP}}/(\text{Wall Width} \times \text{Wall Thickness})$.

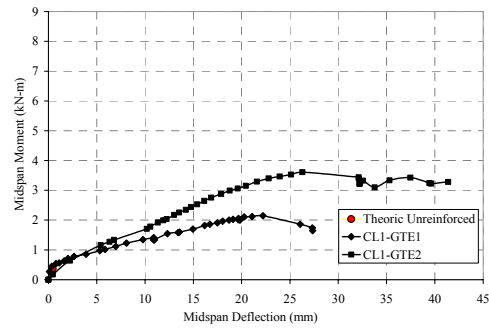
For some of the specimens utilizing carbon or glass FRP rectangular bars, a higher ductility was observed compared with the specimens reinforced with circular bars. In fact, for these specimens the failure was due to the sliding of the bars inside the groove. In these cases, after the failure, the wall could still carry load (because of the friction epoxy paste-bar).

An interesting observation can be underlined for specimens built with a stack pattern bond type. There is not a considerable reduction in the out-of-plane performance by placing the bar in the vertical joints or crossing the masonry blocks.

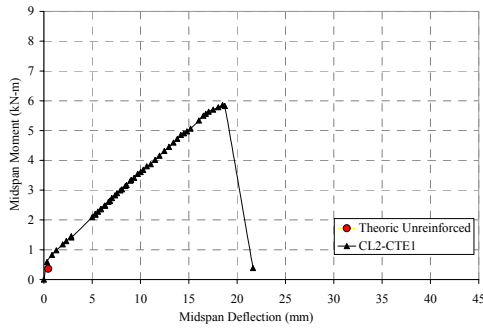
The non-adequate performance of wall CO2-GRE21-SJ is attributed to construction problems. In fact, this wall had a big mortar joint and therefore the epoxy bordered on the mortar and not on the concrete blocks. Therefore it is advisable, as a construction detail, to make grooves bordering the concrete surfaces when bars are placed along the joints.



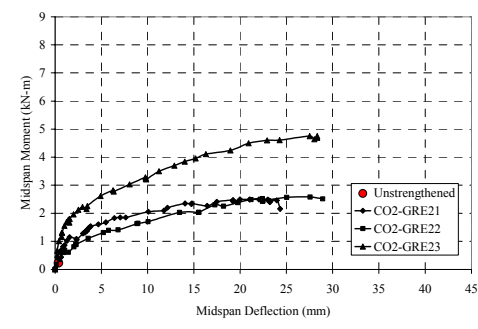
a) Series CO1-GTE



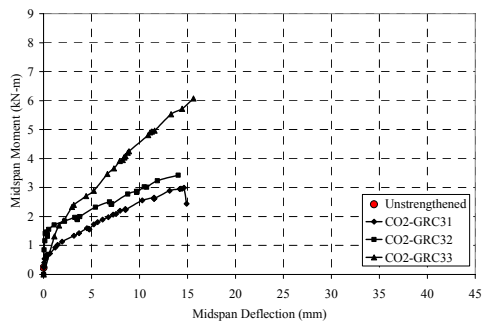
b) Series CL1-GTE



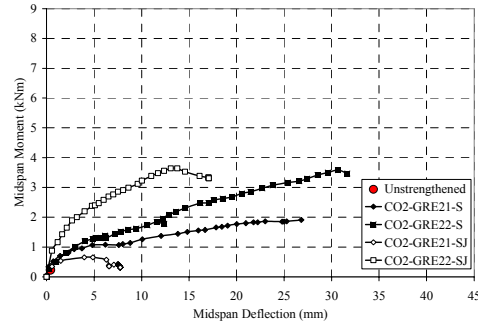
c) Series CL2-CTE



d) Series CO2-GRE2



e) Series CO2-GRC3



f) Series CO2-GRE2x-S

Figure 5 - Moment Versus Midspan Deflection for All the Specimens

Previous Results

Turco, 2002 conducted an experimental investigation on URM walls reinforced with FRP NSM bars. The materials used, the test setup and the dimensions of the masonry panels were the same as the ones described in this paper. In particular a “Type CO2” masonry specimen was used. The differences between the two sets of investigations were in the reinforcement details. Table 5 summarizes the aforementioned results in terms of ultimate bending moment and mode of failure.

It was observed that in the case of strengthening with NSM FRP bar, latex modified cementitious paste-GFRP bar system exhibited a better performance when the size of the groove was approximately 2.25 times the diameter. On the contrary, a groove of 1.5 times the diameter was enough when epoxy paste is used.

Table 4 - Test Results

Specimen Name	Amount of Reinforcement ρ_f ($\times 10^5$)	Ultimate Load kN (kip)	Maximum Bending Moment kN-m (k-ft)	Type of Failure
CO1-GTE1	33	14.7 (3.3)	3.35 (2.47)	Debonding*
CO1-GTE2	67	35.1 (7.9)	8.03 (5.92)	Debonding**
CL1-GTE1	50	9.4 (2.1)	2.16 (1.59)	Debonding**
CL1-GTE2	100	16.0 (3.6)	3.66 (2.70)	Debonding*
CL2-CTE1	50	25.6 (5.8)	5.86 (4.32)	Debonding*
CO2-GRE21	54	11.0 (2.5)	2.52 (1.86)	Debonding**
CO2-GRE22	107	11.5 (2.6)	2.64 (1.95)	Debonding**
CO2-GRE23	161	21.6 (4.9)	4.94 (3.64)	Debonding
CO2-GRC31	136	13.1 (2.9)	2.99 (2.20)	Debonding
CO2-GRC32	272	15.0 (3.4)	3.43 (2.53)	Debonding
CO2-GRC33	408	26.6 (6.0)	6.07 (4.48)	Shear
CO2-GRE21-SJ	50	2.84 (0.64)	0.81 (0.60)	Debonding
CO2-GRE22-SJ	101	16.2 (3.64)	3.43 (2.53)	Debonding
CO2-GRE21-S	50	8.4 (1.9)	1.91 (1.41)	FRP Rupture
CO2-GRE22-S	101	15.8 (3.5)	3.60 (2.66)	FRP Rupture

* Debonding due to sliding of the bar inside the epoxy paste

** Debonding due to splitting of the embedding material

Table 5 - Previous Test Results (Turco, 2002)

Bar Number, Type and Size	Amount of Reinforcement ρ_f ($\times 10^5$)	Square Groove Dimension	Embedment Material	Maximum Bending Moment kNm (k-ft)	Mode of Failure
2#2 GFRP	110	1.5 Bar Diameter 9.5 mm (0.38 in.)	Epoxy	1.68 (1.24)	Debonding
3#2 GFRP	170		Epoxy	2.27 (1.67)	Debonding
1#3 GFRP	120	1.5 Bar Diameter 14.3 mm (0.56 in.)	Epoxy	1.56 (1.15)	Debonding
2#3 GFRP	240		Epoxy	3.93 (2.90)	Shear
3#3 GFRP	360		Epoxy	5.57 (4.11)	Shear
2#2 GFRP	100	2.25 Bar Diameter 14.3 mm (0.56 in.)	Cementitious Paste	2.07 (1.53)	Debonding
3#2 GFRP	170		Cementitious Paste	2.93 (2.16)	Debonding
1#3 GFRP	120	1.5 Bar Diameter 14.3 mm (0.56 in.)	Cementitious Paste	0.94 (0.69)*	Debonding
2#3 GFRP	240		Cementitious Paste	1.64 (1.21)*	Debonding

* Value too low for practical applications

Fortes et al., 2002 conducted an experimental investigation on concrete masonry walls subject to out-of-plane load and reinforced with CFRP rectangular bars. A total of nine walls were tested up to failure. Two reinforcing techniques were compared: CFRP rectangular bars externally bonded to the concrete joints and used as NSM bars. Both reinforcing techniques showed to be effective increasing the ultimate load and its corresponding deflection being the last one the most effective. Table 6 summarizes the aforementioned results in terms of ultimate bending moment and mode of failure.

Table 6- Previous Test Results (Fortes et al., 2002)

Type	Specimen Code	Number of Bars	Embedment Material	Maximum Bending Moment kNm (k-ft)	Mode of Failure
Control Specimens	P1	0	Epoxy	2.73 (2.02)	Tensile Failure of the Masonry at the Joints
	P2	0	Epoxy	3.72 (2.75)	
	P3	0	Epoxy	4.19 (3.09)	
NSM Bars	P4	2	Epoxy	6.36 (4.69)	Debonding
	P5	2	Epoxy	6.29 (4.64)	
	P6	2	Epoxy	7.82 (5.77)	
Externally Bonded	P7	2	Epoxy	7.59 (5.59)	Debonding
	P8	2	Epoxy	7.26 (5.35)	
	P9	2	Epoxy	6.83 (5.04)	

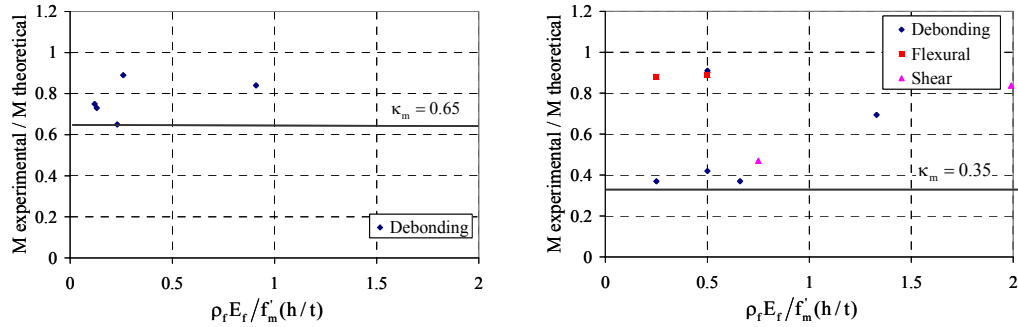
BASIS FOR A DESIGN APPROACH

Of the three modes of failure described, the controlling mode is mostly debonding of the FRP laminate. If a large amount of FRP is provided, shear failure may be observed.

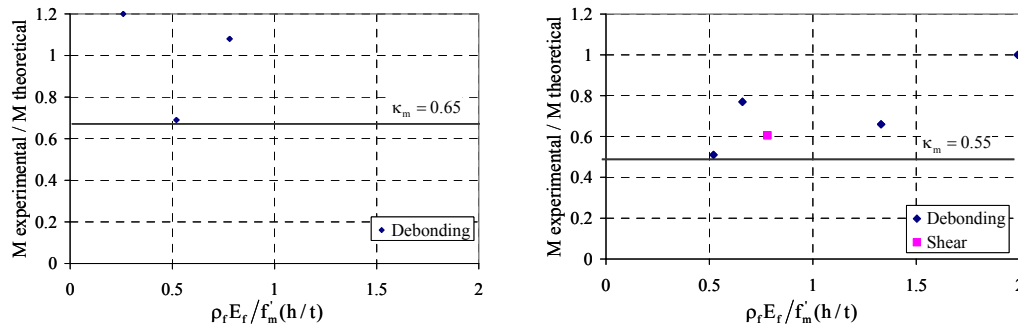
The lower limit ratio $M_{\text{experimental}} / M_{\text{theoretical}}$ has been determined using the same design approach developed by Tumialan et al., 2002. It was defined as a reinforcement ratio ω_f , expressed as $\rho_f E_f / f'_m (h/t)$, for masonry walls strengthened with a variety of FRP reinforcement (E_f is the modulus of elasticity of FRP, f'_m is the masonry compressive strength, and h/t is the wall slenderness ratio).

The theoretical flexural capacity of an FRP strengthened masonry wall can be determined based on strain compatibility, internal force equilibrium, and the controlling mode of failure. Theoretical flexural capacity (i.e. optimum capacity) of the strengthened walls was estimated based on the assumption that no premature failure due to debonding or shear could occur. This means that either rupture of the laminate or crushing of masonry would control the wall behaviour.

For simplicity and similarly to the flexural analysis of RC members, a parabolic distribution was used for compressive stresses in the computation of the flexural capacity of the strengthened walls. According to MSJC 2002 the maximum usable strain ϵ_{mu} was considered to be 0.0035 mm/mm (in/in) for clay masonry, and 0.0025 mm/mm (in/in) for concrete masonry. The tensile strength of masonry was neglected. Figure 6 illustrates the relationship between the experimental-theoretical flexural capacity ratio, and the reinforcement ratio ω_f for URM specimens strengthened with FRP systems.



a) GFRP and CFRP Rectangular Bars – Epoxy System b) GFRP Circular Bars – Epoxy System (dimension of the groove 1.5 the diameter of the bar)



c) GFRP Circular Bars – Epoxy System (dimension of the groove 2.25 the diameter of the bar) d) GFRP Circular Bars – Latex Modified Cementitious Paste (dimension of the groove 2.25 the diameter of the bar)

Figure 6 - $M_{\text{experimental}} / M_{\text{theoretical}}$ versus ω_f

Since the flexural capacity is dependant of the strain developed in the FRP bar, it is reasonable to express the effective strain in the bar, ε_{fe} , as the product $\kappa_m \varepsilon_{fu}$, where κ_m is the bond dependent coefficient and ε_{fu} is the design rupture strain of FRP. Thus, the effective strain in the FRP bar, ε_{fe} , is limited by the strain controlled by debonding:

$$\varepsilon_{fe} \leq \kappa_m \varepsilon_{fu}$$

FRP Rectangular bars: $\kappa_m = 0.65$

FRP Circular Bars Having a Groove 1.5 the Diameter of the Bar : $\kappa_m = 0.35$

FRP Circular Bars Having a Groove 2.25 the Diameter of the Bar: $\kappa_m = 0.55$

These limits are valid for the case of walls not subjected to sustained load. In walls under sustained load such as retaining or basement walls, creep rupture considerations need to be taken into account. Thus, for the case of GFRP, κ_m would be 0.2 (ACI 440.2R-02).

Using this approach it is possible to determine the nominal moment of the section that

multiplied by the ϕ factor of the section must be less or equal to the ultimate moment due to the external applied loads.

CONCLUSIONS

The following conclusion can be drawn from these experimental programs:

1. Flexural strengthening with FRP systems has been proven to remarkably increase of flexural capacity (from 2 to 14 times), strength and pseudo-ductility of URM walls.
2. The test results made possible to identify three basic modes of failure. One, shear failure, related to the parent material (i.e. masonry); and two associated with the reinforcing material, debonding and flexural failure (i.e. rupture of FRP or crushing of the masonry). For large amounts of reinforcement, shear failure was observed to be the controlling mode. For other reinforcement ratios, either FRP rupture or debonding was observed, being the latter the most common.
3. In the case of strengthening with FRP rectangular bars, the sliding of the bar in the epoxy caused an increase in the ductility.
4. Based on experimental data showed in the present investigation and others, it is recommended to consider the maximum usable strain in the FRP Bars as $0.65\varepsilon_{fu}$ for NSM FRP Rectangular Bars utilizing Epoxy Paste and $0.55\varepsilon_{fu}$ for NSM FRP Circular Bars having a groove at least 2.25 times the diameter of the bar and utilizing either Epoxy or Cementitious Paste. The maximum usable strain in the FRP Bars has to be limited to $0.35\varepsilon_{fu}$ for FRP Circular NSM FRP Circular Bars having a groove at least 1.5 times and using Epoxy Paste.

ACKNOWLEDGEMENTS

The support of the National Science Foundation Industry/University Cooperative Research Center at the University of Missouri–Rolla. The authors would also like to acknowledge the support of the Rolla Technical Institute (RTI).

REFERENCES

American Concrete Institute (ACI), Committee 440, “Guide for the Design and Construction of Externally Bonded FRP Systems for Strengthening Concrete Structures”, October 2002.

De Lorenzis L., Nanni A., and La Tegola A., “Flexural and Shear Strengthening of Reinforced Concrete Structures with Near Surface Mounted FRP Rods”, *Proceedings of Third International Conference on Advanced Composite Materials in Bridges and Structures*, Ottawa, Canada, pp. 521-528, 2002.

Fortes A. S., Oliveria J. T. and Barros J. A., “Elementos de Casca em Alvenaria Cerâmica Reforçados com Laminados de Fibras de Carbono”, *VII International Seminar on Structural Masonry for Developing Country*, Belo Horizonte, Brazil, 2002.

Hamid A.A., “Strengthening of Hollow Block Masonry Basement Walls with Plastic Reinforcing Bars”, *The Masonry Society Journal*, 1996.

Masonry Standards Joint Committee, “Building Code Requirements for Masonry Structures, ACI-530-02/ASCE 5-02/TMS 402-02”, *American Concrete Institute, American Society of Civil Engineers, and The Masonry Society*, Detroit, New York, and Boulder, 2002.

Tumialan J.G., Galati N., Namboorimadathil S.M. and Nanni A., “Strengthening of Masonry with FRP Bars”, *ICCI 2002*, San Francisco, CA, June 10-12, 2002

Turco V., Galati N., Tumialan J.G. and Nanni A., “Flexural Strengthening of URM Walls with FRP Systems”, *6 th. International Symposium on Fibre-Reinforced Polymer (FRP) Reinforcement for Concrete Structures (FRPRCS-6)*, Singapore, 2003.